AEGC Australasian Exploration Geoscience Conference Brisbane 2023

Improving predictive modelling of magnetite and gangue mineral content for IOCG and BIF deposits using hyperspectral data and controlled mixtures

Heta Lampinen
CSIRO Mineral Resources
heta.lampinen@csiro.au

Carsten Laukamp
CSIRO Mineral Resources
carsten.laukamp@csiro.au

Bobby Pejcic
CSIRO Mineral Resources
bobby.pejcic@csiro.au

Michael Verrall
CSIRO Mineral Resources
michael.verrall@csiro.au

Ian C Lau
CSIRO Mineral Resources
ian.lau@csiro.au

Jessica Stromberg
CSIRO Mineral Resources
jessica.stromberg@csiro.au

Neil Francis
CSIRO Mineral Resources
neil.francis@csiro.au

SUMMARY

Magnetite is an important ore and gangue mineral in many economic deposits, and the ability to model the modal magnetite abundance from cost-effective data, such as hyperspectral reflectance spectra, has widespread applications. However, magnetite reflectance spectra collected with field and drill core sensors, which are increasingly used by the mineral resources industry, are characterised by very broad and poorly defined diagnostic features. Magnetite content could be modelled indirectly from mixed mineral spectra, but these efforts have been limited by the lack of quantified training datasets of mixed mineral assemblages.

We created two hyperspectral libraries (n=104) of magnetite mixed with quartz, chlorite, and siderite collected from two different wavelength ranges to address this knowledge gap. Mineral ratios and particle size variation, which are important when modelling hyperspectral data, were determined using quantitative X-ray diffraction (QXRD) and scanning electron microscopy with energy-dispersive X-ray spectroscopy (SEM-EDS) analysis. Hyperspectral data were acquired across the visible-near, shortwave, mid to thermal infrared (VNIR-SWIR-MIR-TIR, 380-16669 nm) wavelength range, using HyLogger-3 and Bruker Vertex 80v Fourier transform infrared (FTIR) instruments. Predictive modelling was carried out using CSIRO's The Spectral Geologist (TSG) software partial least squares (PLS) modelling tool, which allows for modelling of one variable (e.g., magnetite wt%) from another (e.g., reflectance spectra) via calibration using a training dataset (magnetite mixture spectral library), and subsequent model validation using other hyperspectral data (e.g., from drillhole) of a similar wavelength range. Use of magnetite mixture PLS calibration enabled prediction of magnetite wt% from drill core VNIR-SWIR data that that matches the Fe_2O_3 assay and magnetic susceptibility detected from the core. We also noted several mineral diagnostic features in the MIR wavelength region, which can provide lower detection limits and an improvement in the accuracy of predictive modelling for magnetite and gangue minerals in the future.

Key words: magnetite, hyperspectral, predictive, modelling, modal mineralogy

INTRODUCTION

Magnetite is a major ore mineral in Banded Iron Formation (BIF)-hosted high-grade iron ore deposits and ubiquitous gangue mineral in iron-oxide copper gold (IOCG) deposits. BIF-hosted high-grade iron ore deposits contain up to 75% magnetite and specular hematite (Davies and Twining, 2018). In IOCGs, magnetite is a crucial part of the ore-forming process, representing up to 20% as a gangue mineral in addition to chlorite, quartz, and carbonate minerals which are also common in BIF-hosted high-grade iron ore deposits (Del Real *et al.* 2021). Demand for a low cost and early-stage ore and gangue mineral quantification process is steadily growing, as this information is crucial for efficient ore processing, which is the part of the mining cycle that consumes the highest amount of energy and has significant impact on the economics of a deposit. With the mining industry rapidly moving towards minimizing environmental impact and energy consumption, predictive modelling methods will play an increasingly critical role in maintaining a social license to operate. All advanced modelling requires large, diverse, well-quantified and consistently collected training data, organized in a manner that can be scaled up as a project proceeds. Hyperspectral data are well established as a cost-effective method for rapid and multi-scale mineral detection from early exploration to ore processing, and its use in predictive modelling has been researched substantially in Australia (Haest *et al.* 2017; Ramanaidou *et al.* 2015; Rodger and Ramanaidou, 2022). However, success in predictive modelling for magnetite has been limited by its rather featureless reflectance spectra within the visible-near (VNIR), shortwave (SWIR), and thermal infrared (TIR)

wavelength ranges, and the lack of quantified mineral mixture training datasets, which could enable indirect detection and quantification of magnetite.

To address this knowledge gap, we created sets of fully quantified and grain-size controlled two-mineral mixtures of magnetite with chlorite, quartz, or siderite, which were analysed using two different hyperspectral instruments across the whole wavelength range from VNIR to TIR (380-16669 nm). Partial least squares (PLS) fitting methods were applied to the mixed magnetite-gangue spectral library to model the actual versus predicted magnetite wt%. The PLS model was validated against drillhole MSDP11 HyLogger-3 data (Stromberg *et al*., 2021) that contains sufficient complimentary data for estimating magnetite wt% prediction success. We present here the resulting spectral libraries and results from the PLS modelling.

MATERIALS AND METHODS

Magnetite samples were prepared from ore concentrate from the Middleback Ranges iron ore camp in South Australia. The quartz, chlorite (clinochlore), and siderite were sourced from the CSIRO Mineral Resources mineral collections. Hematite was removed from the magnetite ore concentrate using a clay separation technique, where red tinted hematite suspended in distilled water was removed and black magnetite deposited at faster rate. All samples were wet sieved to controlled particle size ranges using stainless steel sieves and a constant flow of distilled water. Physically separable contaminants were removed from samples through a combination of hand picking under a binocular microscope and repeated passes with a hand magnet. The particle size and mineral composition for magnetite (<30, 30-45, and 45–90 μm), quartz (<45, 45–90, 90–125, and 125–180 μm), chlorite (<45, 45–90, 90–125, and 125–180 μm) and siderite (<45, 45–90, and 90–125 μm), were confirmed using scanning electron microscopy (SEM) and quantitative X-ray diffraction (QXRD) methods, respectively.

Back-scatter electron images taken using Philips SEM–XL40CP scanning electron microscope at 12.7 mm working distance and 30 kV accelerating voltage. Chemistry for visually different particles in a sample were characterized using non-quantitative energy dispersive x-ray (EDS) point analysis and Bruker Nano Qantax software. For XRD analysis, single mineral samples were hand-ground with ethanol and top loaded to zero background silicon plates. Bruker D4 Endeavor AXS instrument was set to operate with Co radiation, data collection range of 2θ angle from 5 to 90°, with step size of 0.02°, and data collection time of 7 minutes per sample. Initial XRD data analysis and spectrum image acquisition were done using DiffracEVA, and the advanced quantitative analysis was done using SIROQUANT software based on Rietveld method (Rietveld 1967; 1969). Each peak above the background was examined and mineral identification in the analysed samples was done manually in SIROQUANT to ensure that all components present in the multiphase mixtures are identified and accounted for. The XRD results were normalized to 100%.

Mixed magnetite-gangue samples (~2 grams each) were prepared in 10 wt% increments from validated single minerals using a precision scale. Mineral wt% were calculated based on single mineral wt% from QXRD and the measured weight. In total 104 samples were analysed using the HyLogger-3 system (Schodlok *et al*. 2017), and a Bruker Vertex 80v Fourier transform infrared (FTIR) spectrometer.

The HyLogger-3 chip mode which collects three reflectance spectra per sample and are averaged to one when pre-processing spectra from 380-2500 (VNIR-SWIR) and 6000-14500 nm (TIR) wavelength ranges, was used in the data acquisition. HyLogger-3 reflectance spectra were collected from 10 mm area and using a 4 nm spectral resolution within VNIR-SWIR and 25 nm within TIR wavelength range. FTIR spectra were collected from 7500 to 600 cm^{-1} which corresponds to the 1333-16669 nm (SWIR-MIR-TIR) wavelength range. FTIR measurements were made using 256 scans at a spectral resolution of 2 cm^{-1} (resampled to 4 nm in TSG) and a liquid nitrogen cooled mercury cadmium telluride (MCT) detector. Powdered samples were placed in the lower sample port and spectra were measured using a Bruker integrating sphere (A562-G) accessory that has a 10 mm spot size. A background spectrum was recorded on a gold standard reference which had been cleaned in ethanol and dried with Kimwipes tissue (KIMTECH) and high purity nitrogen gas prior to sample measurement. All FTIR spectrometer measurements were undertaken at room temperature (20 ± 2°C) and the infrared spectra have been presented as raw reflectance data.

Hyperspectral data of the two instruments were compiled into two libraries in The Spectral Geologist (TSG) software and calculated mineral wt% resulting from QXRD analysis (single minerals) and mixing ratios were imported in the respective HyLogger-3 and FTIR TSG files. The predictive modelling was carried out using the PLS modelling tool in TSG. PLS creates a linear model that is robust to highly correlated spectral variables, and predicts one variable (e.g. mineral wt%) from multiple correlated variables (e.g. hyperspectral data). The method utilises cross-validation to choose the number of factors incorporated into the model to avoid overfitting, given the volume and inherent variability in the training data. The PLS calibration process for all HyLogger-3 mixed magnetite VNIR-SWIR spectra (n=104) considered up to thirty factors and 12 factors were selected based on the predicted residual sum of squares (PRESS).

The resulting magnetite mixed mineral library PLS model was applied to drillhole MSDP11 VNIR-SWIR wavelength range spectra in TSG. HyLogger-3 data was accessed via AuScope NVCL portal (http://portal.auscope.org.au/). Drillhole MSDP11 (Latitude -32.7316 S, Longitude 135.738 E) intersects skarn intervals in porphyry dominated lithology in the Gawler Range of South Australia (Stromberg *et al*., 2021) and had suitable assay Fe_2O_3% and magnetic susceptibility (KT-9 Kappameter, with measuring range of 9.99 x 10^{-3} to 999 x 10^{-3} SI units) data that could be used for assessing PLS model-based magnetite wt% prediction.

RESULTS

Single minerals labelled as "pure" end members in a series, contain 87, 78 and 61 wt% magnetite in <30, 30-45, 46-90 μm particle sizes (8 wt% hematite in all samples), respectively based on QXRD analysis. All quartz and chlorite particle sizes contain >99 wt% of the mineral, and siderite particle sizes <45, 45-90 and 90-125 μm, contain 97, 95 and 93 wt% siderite, respectively.

Magnetite reflectance spectra are relatively featureless within the VNIR-SWIR and TIR wavelength ranges with overall low reflectance, however; both particle size and mixing ratios with quartz, chlorite and siderite exhibited a consistent linear relationship (Figure 1). Magnetite [$Fe^{3+}(Fe^{2+}Fe^{3+})_2O_4$] VNIR-SWIR spectra had a very broad trough between ~900 nm and ~1200 nm that can be attributed to a combination of Fe^{3+} and Fe^{2+} electronic transitions, respectively (Izawa *et al.* 2019). This 900-1200 nm trough flattens with an increasing magnetite particle size from <30 to 45-90 μm and with decreasing magnetite wt% in mixed samples with quartz and chlorite (Figure 1a). Within TIR wavelength range, the purest magnetite sample spectrum (<30 μm), which was used for the mixed samples, was flat with a slight red slope (Figure 1b). Features in the TIR spectra of 30-45 and 45-90 μm particle size magnetite were caused by the quartz (6-13 wt%) and carbonate (4-9 wt%) impurities in the samples.

Like magnetite, quartz spectra were relatively flat within VNIR-SWIR wavelength range, but there was a subtle trend in mixed samples (Mt-Qz), where the 1200 nm trough flattens with decreasing wt% of quartz in the sample (Figure 1a). In TIR, the two diagnostic quartz features with narrow troughs centred at 8628 and 12650 nm (Hancock *et al.*, 2013) were prominent and decreased with the increasing magnetite wt% in the mixed samples (Figure 1b).

Chlorite spectra had two diagnostic absorptions centred at 2250 and 2350 nm in the VNIR-SWIR reflectance spectra (Bishop *et al.* 2008), of which the former is commonly used for delineating relative chlorite abundance and Mg# composition (Figure 1a, Laukamp *et al.* 2021). These troughs can also be found in dark mica (biotite and phlogopite), so their use requires caution. Chlorite troughs deepen with an increasing particle size and flatten with increasing magnetite wt% in mixed samples (Mt-Chl, Figure 1a). In the TIR, chlorite spectra have a peak centred at ~9800 nm, dubbed as the "triangle of death" by spectral geologists, as it is a common feature in many mineral spectra (e.g., dark micas and amphibole), and is therefore unhelpful for delineating specific mineral groups with certainty (Figure 1b). The 9800 nm peak flattens with an increasing chlorite particle size (pure samples) and increasing magnetite wt% in mixed samples.

Siderite SWIR spectra show an asymmetric absorption feature attributed to CO_3 centred at ~2320 nm, and Fe^{3+} and Fe^{2+} electronic transition associated trough centred between 900-1200 nm (Green and Schodlok, 2016), which deepen with increasing particle size (pure samples) and flatten with increasing magnetite wt% in mixed samples (Mt-Sid, Figure 1a). In the TIR, siderite has two diagnostic peaks centred at ~6500 and 11300 nm and a trough-peak combination centred at ~14200 nm (Figure 1b, Green and Schodlok, 2016). In addition, features attributed to minor quartz impurities (3-7 wt%) in the samples can be seen in the siderite TIR spectra. Siderite peaks and troughs are flatter and erratic in small particle size single mineral samples, which is related to prevalent surface scattering in the TIR wavelength range. As with other mixed samples, siderite features become flatter as the magnetite wt% increases (Figure 1b). The slope that is attributed to magnetite in the TIR wavelength range also increases towards longer wavelengths in all mixed mineral samples with increasing magnetite wt%.

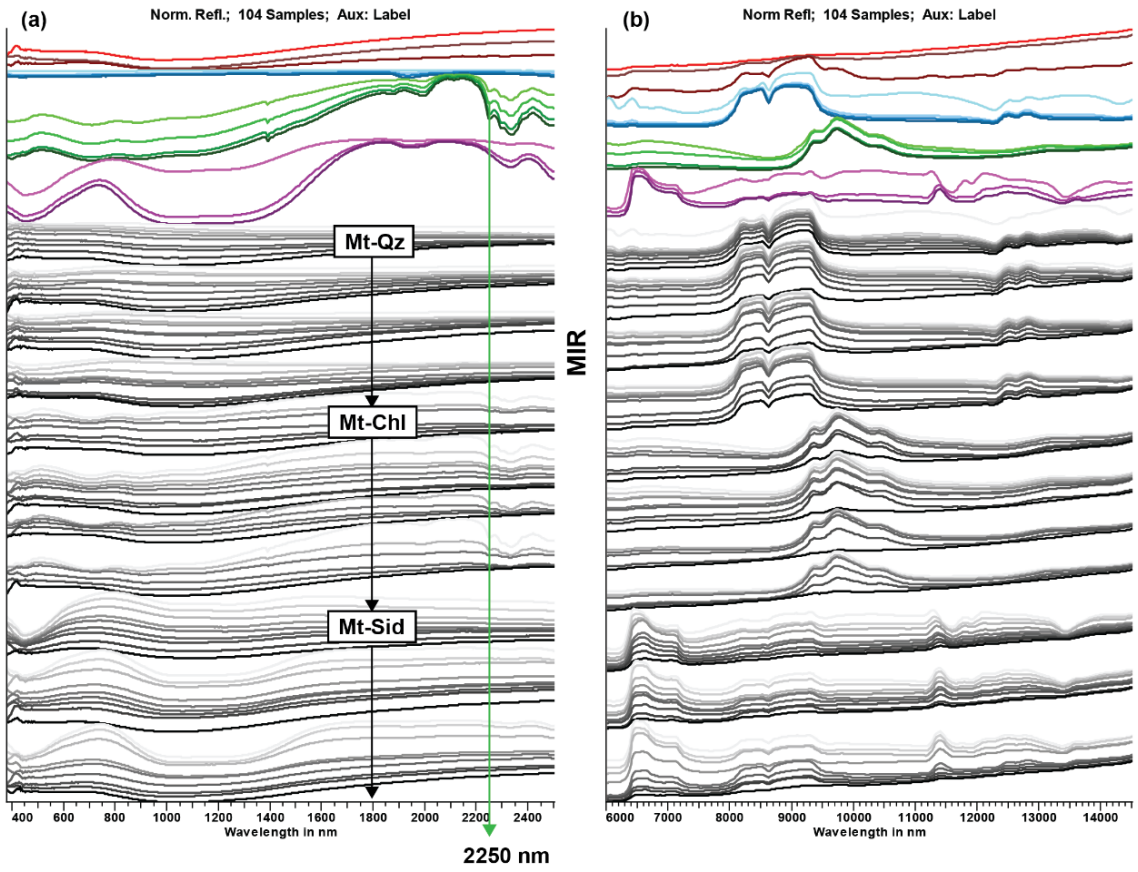

Figure 1. HyLogger-3 spectral library stacked and normalised reflectance spectra within (a) VNIR-SWIR and (b) TIR wavelength range. Reflectance spectra for mixtures between magnetite (light to dark red: <30, 30-45, 45-90 µm), quartz (light to dark blue: <45, 45-90, 90-125, 125-180 µm), chlorite (light to dark green: <45, 45-90, 90-125, 125-180 µm), and siderite (light to dark purple: <45, 45-90, 90-125 µm). Mixed series are presented in grayscale, where sample spectra darkness in figure increases with each 10 wt% increase of magnetite. In mixed series magnetite particle size remains constant <30 µm. Diagnostic chlorite absorption at 2250 nm (discussed in Figure 5) is shown in (a) with a green arrow. Missing mid-infrared wavelength range (MIR, 2500-6000 nm, not captured by the HyLogger-3) is shown in the middle.

Figure 2 summarises the key calibration plots used for creating PLS model for magnetite wt% prediction in TSG from magnetite mixture HyLogger-3 VNIR-SWIR wavelength reflectance spectra. The predicted residual error sum of squares (PRESS) plot was used for determining the number of factors to be applied in the model (n=12, Figure 2a), the final regression coefficient plot was used for viewing which VNIR-SWIR bands (input, i.e., bands along wavelength, total 531) contribute to the model most (Figure 2b). Cross-validation actual vs predicted magnetite wt% (Figure 2c) shows the PLS model fit within the calibration data set (i.e., magnetite mixture data). The variance indicated by root-mean-square-error (RMSE) is tighter compared to what would be expected on independent data. RMSE is a frequently used metric for comparing the predictive error of different models created and validated on the same dataset. Smaller RMSE generally suggests a better predictive model. However, it is not meaningful to use RMSE to compare models trained and tested on different datasets. The cross-validation actual vs predicted magnetite wt% plot coloured by mineral labels (Figure 2d) shows that magnetite wt% was slightly more overpredicted in mineral mixtures with quartz and siderite, that are typically best delineated from TIR wavelength range spectra, whereas chlorite mixtures show no obvious trend.

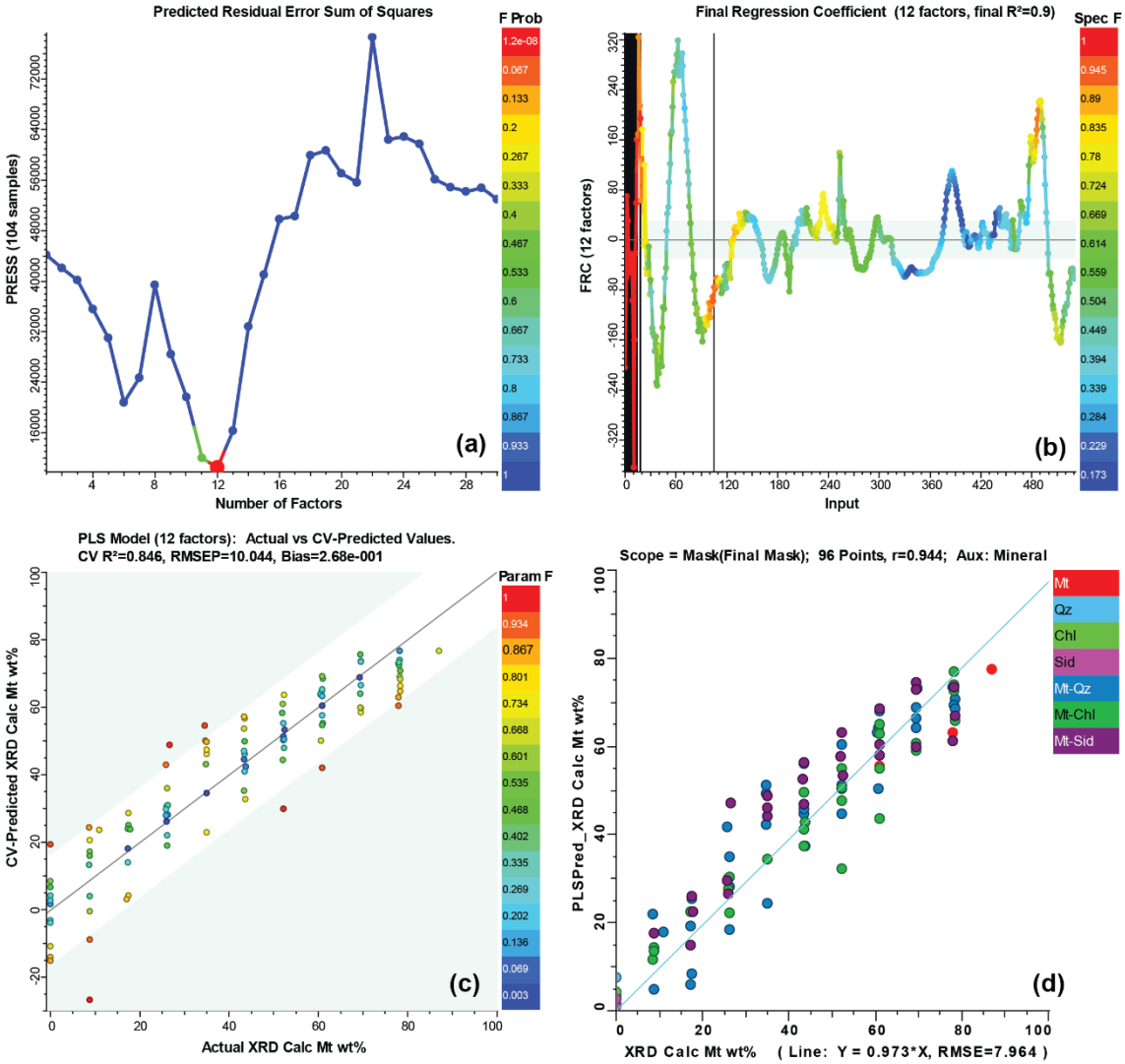

Figure 2. HyLogger-3 magnetite mixture VNIR-SWIR spectral library PLS modelling process in TSG: (a) selection of number of factors, (b) final regression coefficient plot, (c) cross-validation actual versus predicted magnetite wt% in the samples, and (d) cross-validation actual magnetite wt% versus predicted magnetite wt% coloured by mineral labels showing slight over prediction for magnetite in mixtures with quartz and siderite that are better delineated from TIR wavelength reflectance spectra.

The magnetite mixture spectral library PLS model applied to drillhole MSDP11 HyLogger-3 data enabled prediction of magnetite wt% from VNIR-SWIR wavelength range spectra (Figure 3a, d). The predicted high magnetite wt% between 320-380 and 410-425 m drillhole depth, coincide with a very high magnetic susceptibility (Figure 4b). Further, the predicted magnetite wt% follow Fe_2O_3% contour (Figure 4c).

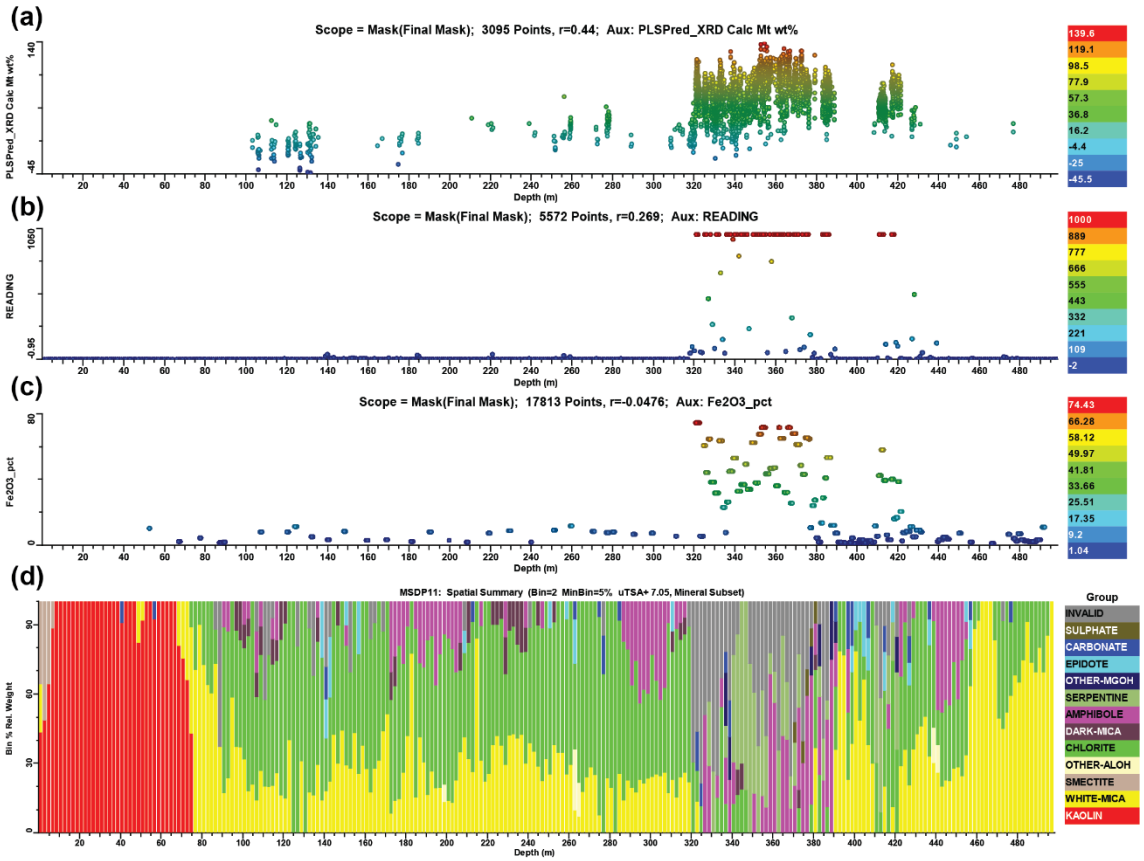

Figure 3. Drillhole MSDP11 HyLogger-3 downhole plot demonstrating successful (a) prediction of magnetite wt% using magnetite mixture VNIR-SWIR spectral library PLS calibration model. (b) Magnetic susceptibility (x 10^{-3} SI units), (c) Fe_2O_3% assay data and (d) user verified TSA mineral group match based on SWIR wavelength range spectra (Stromberg *et al.* 2021) corroborate with PLS model-based magnetite wt%.

Several mineral specific features can be seen within MIR wavelength range reflectance spectra that was collected from magnetite mixture samples by means of FTIR (Figure 4). All particle size magnetite samples have two peaks with a narrow trough in the middle, centred at ~4250 nm, and these features can be observed in mixed samples even in low magnetite wt% (Figure 4). Our early work on iron oxide MIR reflectance spectra indicates that ~4250 nm features are partly due to atmospheric carbon dioxide and iron oxide (magnetite/hematite/goethite) overtones. Quartz sample reflectance spectra have two broad peaks with narrow trough centred at ~4670 nm (Laukamp *et al.* 2021), and numerous other features that are yet to be investigated (Figure 4). The chlorite sample MIR reflectance spectra contain a feature at 2830 nm, whereas the siderite sample MIR spectra contain several features centred at ~2550 (CO_3), 3500, and 4000 nm (Figure 4). Similar to the VNIR-SWIR and TIR wavelength range (Figure 1), flattening of mineral specific features in mixed sample MIR wavelength spectra is proportionally related to magnetite wt% in the sample (Figure 4).

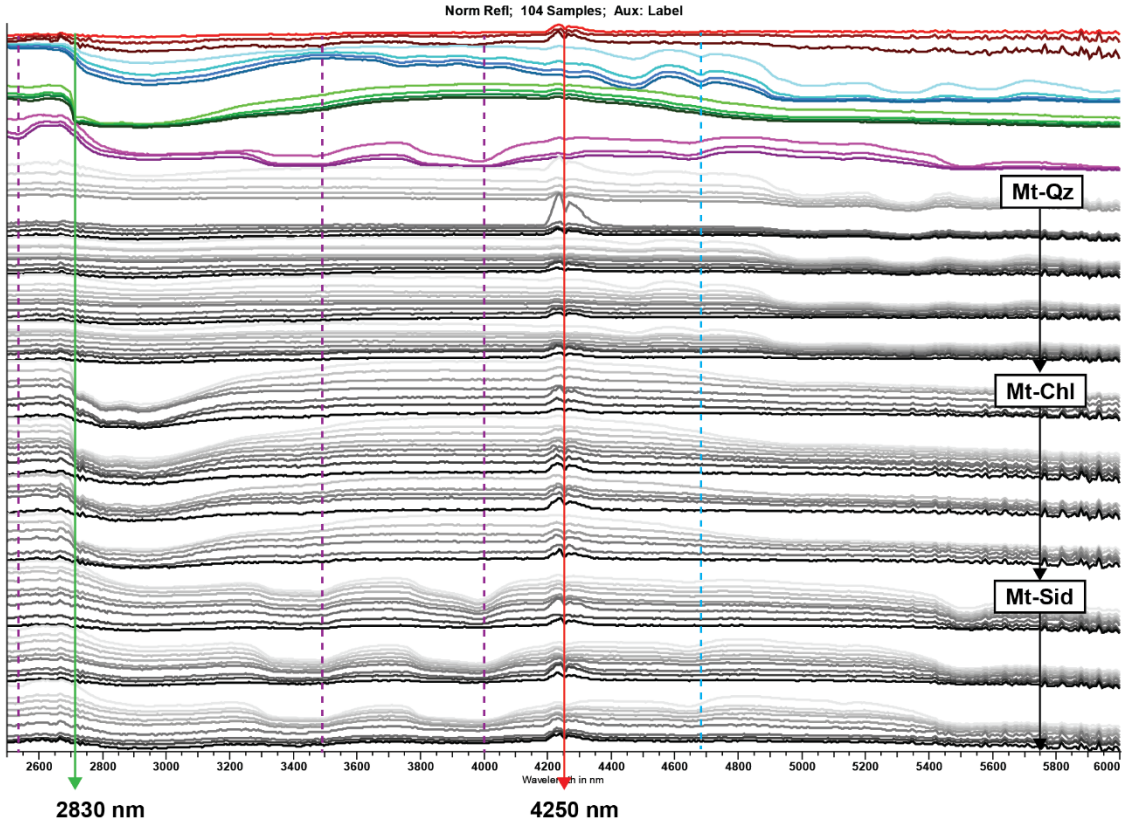

Figure 4. FTIR mid-infrared spectral library stacked and normalised reflectance spectra for mixtures between magnetite, quartz, chlorite, and siderite in a series as in Figure 1. Chlorite absorption at ~2830 nm (discussed in Figure 5) and magnetite associated features (2 peaks and 1 trough) centred ~4250 nm are shown with green and red arrows, respectively. Some of the diagnostic MIR absorptions for siderite (purple) and quartz (blue) are shown with dashed lines.

We demonstrate the added value of the MIR wavelength region for the predictive quantitative modelling of minerals by using chlorite as an example as chlorite is an important alteration mineral in many ore systems. Chlorite associated features within VNIR-SWIR and TIR wavelength range are shared by many other minerals that often occur with chlorite (carbonate, biotite, amphiboles), which adds to uncertainty and false positives in predictive modelling. Chlorite delineation based on absorption feature depth at ~2250 nm, demonstrated in Figure 5a using 125-180 μm particle size magnetite-chlorite mixture series (collected using the Vertex 80v FTIR spectrometer), yields an approximate detection limit of >70 wt% for chlorite within VNIR-SWIR wavelength range data. When using similar technique for the chlorite feature at 2830 nm within MIR wavelength range, chlorite content above 30 wt% can be detected (Figure 5b).

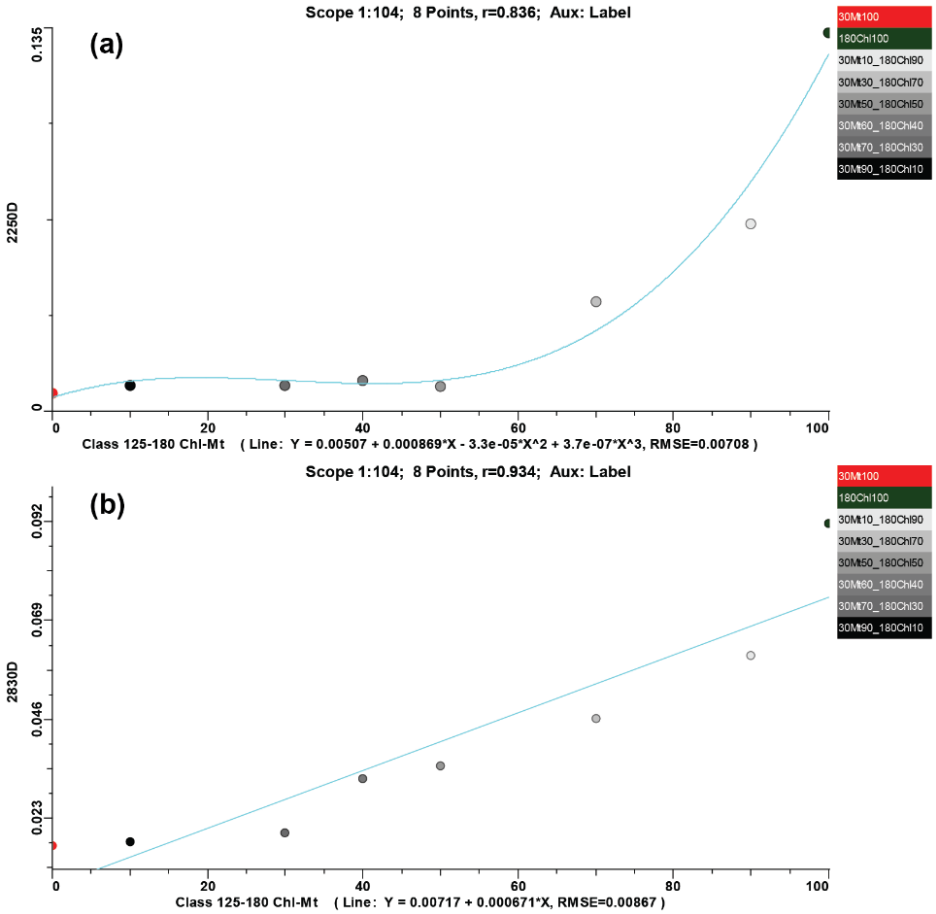

Figure 5. Example of correlation between depth of chlorite absorption (y-axis) at (a) 2250 nm in SWIR (Figure 1) and (b) 2830 nm in MIR (Figure 4) and chlorite weight percentage (x-axis) in 125-180 µm particle size series. Chlorite is detected after 60 wt% within SWIR and after 30 wt% within MIR. Hyperspectral data with both features should enable much more precise predictive modelling.

CONCLUSION

Predictive modelling for quantitative mineralogy from hyperspectral data is generally best carried out using site specific training datasets that are acquired using the same instrument, however, this is not always practical or possible in an exploration or ore characterization setting. In these cases, a generic but well characterised mixed mineral spectral library can be a valuable substitute or addition to a predictive modelling workflow. This work presents such a dataset and describes the reflectance spectra characteristics of physically mixed magnetite – quartz/chlorite/siderite pairs in two spectral libraries. It also provides an example of early predictive modelling results using PLS tool in TSG for drill core dataset. Results from PLS modelling suggest that magnetite wt% can be predicted relatively accurately from any routinely collected VNIR-SWIR data when using the spectral library calibration file. Further, mixing ratio related linear behaviour and magnetite diagnostic features in MIR wavelength suggest that modelling results using the full wavelength range from VNIR to TIR could yield, not only accurate, but precise results. This is an important step forward in this field and provides a proof of concept for developing applications and facilitating uptake of new and emerging sensor technologies, including handheld instruments (e.g., Agilent 4300) and drill core scanners (e.g., HyLogger-4) which have MIR capabilities.

We will continue to improve predictive modelling applications of mixed spectral libraries using the AuScope National Virtual Core Library (NVCL) HyLogger-3 data collected by Australian geological surveys from BIF and IOCG deposit types. In the near future many of the surveys will transition to using HyLogger-4 systems, which include the MIR wavelength region, making full wavelength range datasets available for testing predictive modelling.

ACKNOWLEDGMENTS

The authors would like to thank James Manuel and Eric Ramanaidou (CSIRO) for facilitating access to the magnetite concentrate and Andrew Rodger (at the time CSIRO, currently BHP) for providing advice regarding predictive modelling. This work has been fully funded by the CSIRO Mineral Resources Discovery Program.

REFERENCES

Bishop, J.L. Lane, M.D., Dyar, M., and Brown, A.J., 2008, Reflectance and emission spectroscopy study of four groups of phyllosilicates: smectites, kaolinite-serpentines, chlorites and micas: Clay Minerals, 48, 35-54.
Green, D., and Schodlok M., 2016, Characterisation of carbonate minerals from hyperspectral TIR scanning using features at 14 000 and 11 300 nm: Australian Journal of Earth Sciences, 63 (8), 951-957.

Davies, M., and Twining, M., 2018, Magnetite: South Australia's resource potential, MESA Journal 86 (1), 30-44.

Del Real, I., Reich, M., Simon, A.C., Deditius, A., Barra, F., Rodríguez-Mustafa, M.A., Thompson, J.F.H, and Roberts, M., 2021, Formation of giant iron oxide-copper-gold deposits by superimposed, episodic hydrothermal pulses: Nature Communications Earth and Environment, 2:192, 1-9.

Haest, M., Mittrup, D., Edwards, L., 2017, Infrared spectroscopy in BHP Billiton iron ore with a focus on in-mine infrared sensing: Iron Ore Conference 2017, 24.-26.7.2017, Perth, Australia, Extended Abstracts, 7.

Hancock, E.A., Green, A.A., Huntington, J.F., Schodlok, M.C., and Whitbourn, L.B., 2013, HyLogger-3: Implications of adding thermal-infrared sensing: Geological Survey of Western Australia, Record 2013/3, 24p.

Izawa, M.R.M, Cloutis, E.A., Rhind, T., Mertzman, S.A., Applin, D.M, Stromberg, J.M., and Sherman, D.M., 2019, Spectral reflectance properties of magnetites: Implications for remote sensing: Icarus, 319, 525-539.

Laukamp, C., Rodger, A., LeGras, M., Lampinen, H., Lau, I.C., Pejcic, B., Stromberg, J., Francis, N., and Ramanaidou, E., 2021, Mineral Physicochemistry Underlying Feature-Based Extraction of Mineral Abundance and Composition from Shortwave, Mid and Thermal Infrared Reflectance Spectra: Minerals 11, 347.

Ramanaidou, E., Wells, M., Lau, I., and Laukamp, C., 2015, Characterization of iron ore by visible and infrared reflectance and, Raman spectroscopies: Chapter 6, Iron Ore, Elsevier.

Rietveld, H.M., 1967, Line Profiles of Neutron Powder-Diffraction Peaks for Structure Refinement: Acta Crystallographica, 22, 151-152.

Rietveld, H.M., 1969, A profile refinement method for nuclear and magnetic structures: Journal of Applied Crystallography, 2, 65-71.

Rodger, A., and Ramanaidou, E., 2022, Deconstructing the Iron Boomerang—Quantitative Predictions of Hematite, Ochreous, and Vitreous Goethite Mixtures: Minerals, 12(3), 381.

Schodlok, M.C., Green, A., and Huntington, J.A., 2016, Reference Library of Thermal Infrared Mineral Reflectance Spectra for the HyLogger-3 Drill Core Logging System: Australian Journal of Earth Sciences, 63, 941–949.

Stromberg, J.M., Gordon, G., Fabris, A., Laukamp, C., 2021, HyLogger Case Study: South Gawler Craton (MSDP11) Pt. 1 Geological Context and Introduction to NVCL Datasets: CSIRO Report EP208173, Australia.